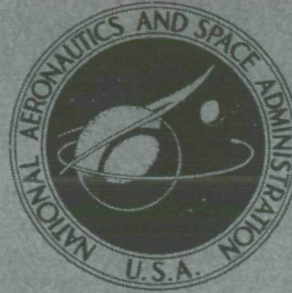


NASA TECHNICAL  
MEMORANDUM



NASA TM X-2515

NASA TM X-2515

CASE FILE  
COPY

TURBULENT-BOUNDARY-LAYER DEVELOPMENT  
ON A MOVING GROUND BELT  
OF ROUGH TEXTURE

*by Alan T. Roper and Garl L. Gentry, Jr.*

*Langley Research Center*

*Hampton, Va. 23365*

NATIONAL AERONAUTICS AND SPACE ADMINISTRATION • WASHINGTON, D. C. • APRIL 1972



Page Intentionally Left Blank

1. Report No. NASA TM X-2515	2. Government Accession No.	3. Recipient's Catalog No.	
4. Title and Subtitle TURBULENT-BOUNDARY-LAYER DEVELOPMENT ON A MOVING GROUND BELT OF ROUGH TEXTURE		5. Report Date April 1972	
		6. Performing Organization Code	
7. Author(s) Alan T. Roper, Rose-Hulman Institute of Technology; and Garl L. Gentry, Jr.		8. Performing Organization Report No. L-7845	
		10. Work Unit No. 136-63-02-07	
9. Performing Organization Name and Address  NASA Langley Research Center Hampton, Va. 23365		11. Contract or Grant No.	
		13. Type of Report and Period Covered Technical Memorandum	
12. Sponsoring Agency Name and Address  National Aeronautics and Space Administration Washington, D.C. 20546		14. Sponsoring Agency Code	
15. Supplementary Notes			
16. Abstract  <p>The equations presented can be used to predict the shape factor and the ratio of the momentum thickness to the relative momentum thickness with reasonable accuracy for a moving ground belt provided that the stationary quantities are known and the two following basic approximations are valid: (1) Shape factor based upon velocity relative to the ground belt is nearly independent of the ratio of belt velocity to free-stream velocity and (2) the ratio of moving-belt momentum thickness to stationary-belt momentum thickness is independent of the coordinate measured in the streamwise direction. In addition, the integral quantities, momentum thickness and displacement thickness, can be predicted for the moving ground belt by using an empirically determined polynomial whose coefficients will change with different belt roughnesses.</p>			
17. Key Words (Suggested by Author(s))  Boundary-layer parameters Moving-belt ground plane		18. Distribution Statement  Unclassified - Unlimited	
19. Security Classif. (of this report) Unclassified	20. Security Classif. (of this page) Unclassified	21. No. of Pages 26	22. Price* \$3.00

# TURBULENT-BOUNDARY-LAYER DEVELOPMENT ON A MOVING GROUND BELT OF ROUGH TEXTURE

By Alan T. Roper\* and Garl L. Gentry, Jr.  
Langley Research Center

## SUMMARY

Equations are presented which can be used to predict the shape factor and the ratio of the momentum thickness to the relative momentum thickness with reasonable accuracy for a moving ground belt of rough texture provided that the stationary quantities are known and the two following basic approximations are valid: (1) Shape factor based upon velocity relative to the ground belt is nearly independent of the ratio of belt velocity to free-stream velocity and (2) the ratio of moving-belt momentum thickness to stationary-belt momentum thickness is independent of the coordinate measured in the streamwise direction. In addition, the integral quantities, momentum thickness and displacement thickness, can be predicted for the moving ground belt by using an empirically determined polynomial whose coefficients will change with different belt roughnesses.

## INTRODUCTION

Considerable interest has been displayed recently in tube vehicle systems. Fundamental to the design of such a system is the near-field fluid behavior, an important part of which is the boundary-layer development on both the vehicle and the tube wall. The wall layer is analogous to a boundary layer developing over a moving ground plane traveling at a velocity equal to the free-stream velocity. The moving-belt ground plane in the Langley 300-MPH 7- by 10-foot tunnel has provided an invaluable source of empirical information for such layers. The problem of fluid behavior is of interest in other areas; for example, in the development of boundary layers behind a moving expansion wave such as in a Ludwig tube type tunnel.

All present methods of turbulent-boundary-layer calculation rely heavily upon empirical information. Since no significant body of such information exists for the moving ground plane, any useful method of prediction must originate from stationary-ground-plane

---

\*Professor, Department of Mechanical and Aerospace Engineering, Rose-Hulman Institute of Technology, Terre Haute, Indiana.

methods. The purpose of this study is to find a way to accomplish the transition from stationary- to moving-ground-plane methods.

## SYMBOLS

The units used for the physical quantities in this report are given both in International System of Units (SI) and in the U.S. Customary Units. Measurements and calculations were made in the U.S. Customary Units.

$c_f$	local skin-friction coefficient
$C_f$	total skin-friction coefficient
$g(R)$	empirically determined polynomial (see eq. (14))
$H$	shape factor, $\delta^*/\theta$
$r$	exponent of $u$ (see eq. (6))
$R$	velocity ratio, $V_B/U$
$u$	local x-component of velocity, m/sec (ft/sec)
$U$	free-stream x-component of velocity, m/sec (ft/sec)
$v$	local y-component of velocity, m/sec (ft/sec)
$V_B$	ground-belt speed, m/sec (ft/sec)
$x$	coordinate measured in streamwise direction, cm (in.)
$x'$	dummy variable
$y$	coordinate measured normal to ground plane, cm (in.)
$\delta$	boundary-layer thickness
$\delta^*$	displacement thickness

$\theta$  momentum thickness

$\rho$  density, kg/m<sup>3</sup> (slugs/ft<sup>3</sup>)

$\tau$  shearing stress

Subscript:

o a stationary ground-belt quantity or at  $y = 0$

A tilde ( $\sim$ ) over a symbol indicates a relative quantity or one based upon velocity relative to the ground belt.

## ANALYSIS

### Experimental Data

Data analyzed in this study were taken from boundary-layer velocity profiles reported in reference 1. These velocity profiles were obtained in the 5.18-meter (17-ft) test section of the Langley 300-MPH 7- by 10-foot tunnel, which was fitted with a moving-belt ground board (ref. 2). Velocity profiles were measured at a free-stream dynamic pressure of 526.7 N/m<sup>2</sup> (11 lbf/ft<sup>2</sup>), a free-stream velocity of 29.26 m/sec (96 ft/sec), and a Reynolds number per unit length of  $20.1 \times 10^5$  per meter ( $6.1 \times 10^5$  per ft) at stations 0.41, 1.37, and 2.62 meters (16, 54, and 103 in.) aft of the leading edge of the belt, as illustrated in figure 1. Ratios of  $V_B/U$  of approximately 0, 0.26, 0.52, 0.78, and 1.00 were used in the investigation. Velocity-profile data obtained from original data plots (ref. 1) are listed in table I, and a summary of gross boundary-layer parameters from velocity profiles for stations 1.37 and 2.62 meters (54 and 103 in.) are presented in table II. No corrections have been applied to the data.

The belt installed during the tests was made of a woven woolen material with a feltlike surface. The behavior of the boundary layer over such a rough texture will differ from what would be expected over a smooth surface. To determine the effect of the roughness of the belt, a smooth thin metal plate was placed over the belt, and the boundary-layer profile was measured at a station 1.42 meters (55.90 in.) from the leading edge of the belt at  $V_B = 0$  (ref. 2). The metal plate was removed and another boundary-layer profile was taken over the belt at the identical location. The results presented in figure 2 show that the boundary layer is definitely thicker when the woolen belt is used.

In all tests, the tunnel boundary layer was bled off at the leading edge of the belt, and the belt layer is assumed to start from zero thickness at that point. In practice,

complete removal of the tunnel boundary layer was not achieved. (See  $R = 1.0$  profiles in table I.) Additional disturbances were caused at the leading edge by the slot (between the suction plate and the belt) and the natural entrainment of air from this slot by the belt motion. Since these disturbances, as well as the transient conditions associated with the initial stages of the boundary-layer development, are most strongly apparent at the station nearest the leading edge (fig. 9(a), ref. 1), only stations 1.37 and 2.62 meters (54 and 103 in.) were included in the analysis of this report. (For convenience, these stations will be designated as stations 1.37 and 2.62 throughout the remainder of this report.) The data at these stations are shown in figure 3 in the form of relative velocity ratio

$$\frac{\tilde{u}}{\tilde{U}} = \frac{u - V_B}{U - V_B} \quad (1)$$

as a function of  $y$ .

Summary charts for the variation of  $x$  with the boundary-layer thickness  $\delta$  and the integral parameters

$$\delta^* = \int_0^\infty \left(1 - \frac{u}{U}\right) dy \quad (2a)$$

$$\theta = \int_0^\infty \frac{u}{U} \left(1 - \frac{u}{U}\right) dy \quad (2b)$$

$$H = \frac{\delta^*}{\theta} \quad (2c)$$

$$C_f = \frac{1}{x} \int_0^x c_f dx' = 2 \frac{\theta}{x} \quad (2d)$$

are presented in figure 4.

If the absolute velocities in equations (2a), (2b), and (2c) are replaced by relative velocities, the following relative integral parameters are obtained:

$$\tilde{\delta}^* = \int_0^\infty \left(1 - \frac{\tilde{u}}{\tilde{U}}\right) dy \quad (3a)$$

$$\tilde{\theta} = \int_0^\infty \frac{\tilde{u}}{\tilde{U}} \left(1 - \frac{\tilde{u}}{\tilde{U}}\right) dy \quad (3b)$$

$$\tilde{H} = \frac{\tilde{\delta}^*}{\tilde{\theta}} \quad (3c)$$

The integral parameters listed in equations (2) and (3) were determined from the measured data. Their variation with the ratio  $R = V_B/U$  is presented in figure 5.

Stationary-ground-plane integral parameters can be written in terms of relative boundary-layer parameters by using the relations

$$\delta^* = (1 - R)\tilde{\delta}^* \quad (4a)$$

$$\theta = (1 - R)^2\tilde{\theta} + R(1 - R)\tilde{\delta}^* \quad (4b)$$

$$H = \frac{\tilde{H}}{1 + R(\tilde{H} - 1)} \quad (4c)$$

### Theoretical Considerations

The boundary-layer equations for two-dimensional incompressible flow over a flat plate are

$$u \frac{\partial u}{\partial x} + v \frac{\partial u}{\partial y} = \frac{1}{\rho} \frac{\partial \tau}{\partial y} \quad (5a)$$

$$\frac{\partial u}{\partial x} + \frac{\partial v}{\partial y} = 0 \quad (5b)$$

The  $r$ th moment of the momentum equation can be generated in its usual form as

$$\frac{\partial}{\partial x} (u^{r+2}) + \frac{\partial}{\partial y} (vu^{r+1}) = (r + 1) \frac{u^r}{\rho} \frac{\partial \tau}{\partial y} \quad (6)$$

Application of the continuity equation and the boundary conditions

$$u(x, 0) = V_B$$

$$u(x, \delta) = U$$

$$v(x, 0) = 0$$

permits the integration of equation (6) and gives

$$\frac{\partial f_r}{\partial x} = e_r \quad (7)$$



where

$$f_r = \int_0^\infty \frac{u}{U} \left[ 1 - \left( \frac{u}{U} \right)^{r+1} \right] dy \quad (8a)$$

$$e_r = -(r + 1) \int_0^\infty \left( \frac{u}{U} \right)^r \frac{\partial}{\partial y} \left( \frac{\tau}{\rho U^2} \right) dy \quad (8b)$$

The integral form of the moment equation is obtained from equations (5) and (6) by setting  $r = 0$ . The result is

$$\frac{d\theta}{dx} = \frac{\tau_o}{\rho U^2} = \frac{C_f}{2} \quad (9)$$

Equation (9) remains unchanged from the stationary-ground-plane expression, which implies that the form of the dependence of local skin-friction coefficient upon  $\theta$  remains unchanged when the ground belt is set in motion.

#### Proposed Solution

The data presented in figure 5(d) suggest that  $\tilde{H}$  is more nearly independent of  $R$  than any of the other parameters (maximum observed variation being approximately 7 percent). For stations 1.37 and 2.62, the following approximation is made:

$$\tilde{H}(x, R) \approx H(x, 0) = H_o(x) \quad (10)$$

Equation (4b) can be rewritten as

$$\frac{\theta}{\tilde{\theta}} \approx (1 - R)^2 + R(1 - R)H_o \quad (11)$$

A comparison between values predicted by equation (11) and measured data is presented in figure 6. Agreement is very good, with a maximum deviation on the order of 3 percent.

By means of the same approximation, equation (4c) can be rewritten as

$$H \approx \frac{H_o}{1 + R(H_o - 1)} \quad (12)$$

This approximation (also shown in fig. 6) is satisfactory and has a maximum deviation from the measured data of approximately 5 percent. Other ratios could be produced in

the same manner but are not particularly useful. It is interesting to note, however, that equation 4(a) implies that  $\delta^*/\tilde{\delta}^*$  is independent of  $x$  and stationary-ground-plane conditions.

Equations (10) to (12) partly describe the behavior of the moving-ground-plane boundary layer. It is desirable, however, to be able to predict the parameters  $\theta$  and  $\delta^*$  themselves for  $R \neq 0$ .

Examination of measured values of the ratio  $\theta/\theta_0$  (fig. 7) reveals a much weaker dependency upon  $x$  than upon  $R$ . Therefore, on the basis of existing data, the approximation

$$\frac{\theta}{\theta_0} = g(R) \quad (13)$$

appears to be valid, where the function  $g(R)$  can be represented by a polynomial in  $R$ . Accordingly, the expression

$$g(R) = (1 - R)[1 - 0.411R + 0.013R(1 + R)] \quad (14)$$

was selected to represent the data. The values of the coefficients in the expression for  $g(R)$  may change for different ground-belt roughnesses, however.

If approximation (14) is combined with approximation (13), the result is as follows:

$$\theta = (1 - R)(1 - 0.398R + 0.013R^2)\theta_0 \quad (15)$$

A comparison of values of  $\theta$  predicted from equation (15) with those obtained by experiment is presented in figure 8. The agreement between predicted and measured values is very good.

The displacement thickness  $\delta^*$  can be obtained from the product of equations (12) and (15) as

$$\delta^* = \frac{H_0(1 - R)(1 - 0.398R + 0.013R^2)\theta_0}{1 + R(H_0 - 1)} \quad (16)$$

Values of  $\delta^*$  computed from equation (16) are compared with experimental data in figure 9. Again, the agreement between predicted and measured values is very good.

The validity of the equations obtained in this study rests ultimately upon the following approximations:  $\tilde{H}$  is nearly independent of  $R$  and  $\theta/\theta_0$  is nearly independent of  $x$ . Further experimental information (ref. 3) indicates that the numerical values of the coefficients in the expression for  $g(R)$  (eq. (14)) change for the smooth-belt case. Too little information exists at the present time, however, to speculate as to the universality of the new coefficients.

### CONCLUDING REMARKS

The equations presented can be used to predict the shape factor and the ratio of the momentum thickness to the relative momentum thickness with reasonable accuracy for a moving ground belt provided that the stationary quantities are known and the two following basic approximations are valid: (1) Shape factor based upon velocity relative to the ground belt is nearly independent of the ratio of belt velocity to free-stream velocity and (2) the ratio of moving-belt momentum thickness to stationary-belt momentum thickness is independent of the coordinate measured in the streamwise direction. In addition, the integral quantities, momentum thickness and displacement thickness, can be predicted for the moving ground belt by using an empirically determined polynomial whose coefficients will change with different belt roughnesses.

Langley Research Center,  
National Aeronautics and Space Administration,  
Hampton, Va., March 3, 1972.

### REFERENCES

1. Turner, Thomas R.: Wind-Tunnel Investigation of a 3/8-Scale Automobile Model Over a Moving-Belt Ground Plane. NASA TN D-4229, 1967.
2. Turner, Thomas R.: A Moving-Belt Ground Plane for Wind-Tunnel Ground Simulation and Results for Two Jet-Flap Configurations. NASA TN D-4228, 1967.
3. Roper, Alan T.; and Gentry, Garl L., Jr.: Analysis of a Turbulent Boundary Layer Over a Moving Ground Plane. NASA TN D-6788, 1972.

TABLE I. - DATA FROM BOUNDARY-LAYER SURVEYS

(a) Station 0.41 meter (16 in.)

y		u/ $\bar{U}$ for R equal to -				
cm	in.	0	0.27	0.54	0.82	1.00
0.254	0.10	0.605	0.592	0.792	0.873	0.933
.584	.23	.756	.827	.882	.922	.947
1.016	.40	.895	.943	.961	.976	.986
1.346	.53	.975	.988	.995	.995	1.000
1.778	.70	.988	.995	1.000	1.000	
2.489	.98	1.000	1.000			
5.080	2.00	1.000				

(b) Station 1.37 meters (54 in.)

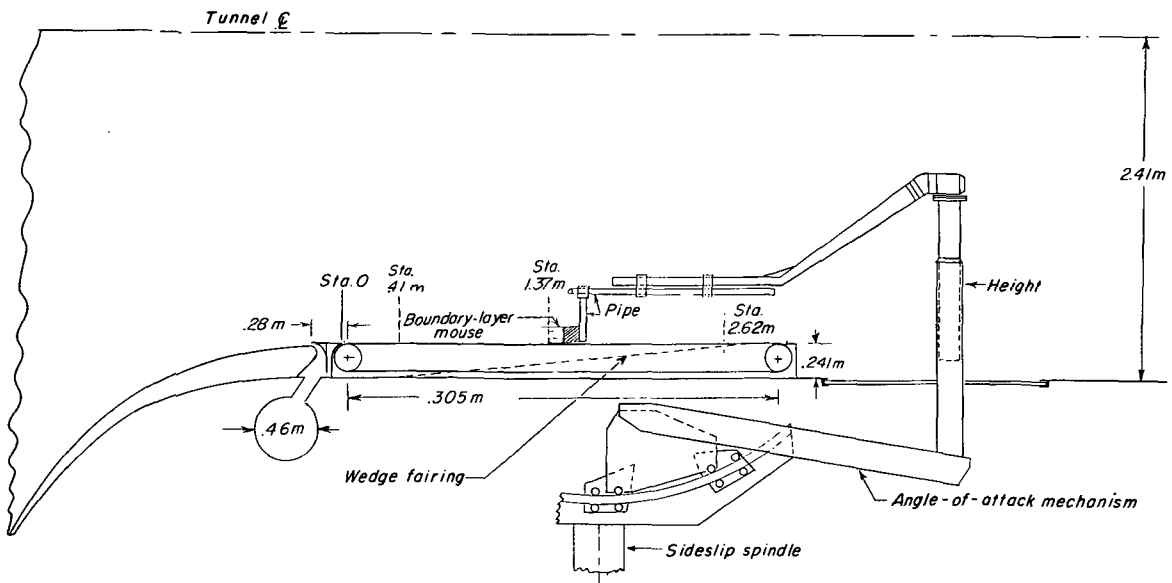
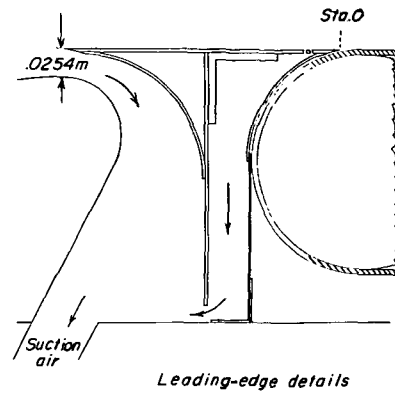
y		u/ $\bar{U}$ for R equal to -				
cm	in.	0	0.26	0.52	0.78	1.04
0.254	0.10	0.510	0.658	0.775	0.906	0.995
.559	.22	.602	.728	.835	.930	.982
1.016	.40	.689	.807	.894	.959	.988
1.321	.52	.744	.858	.932	.972	.993
1.778	.70	.796	.901	.958	.995	.998
2.464	.97	.883	.962	.990	.999	1.000
3.099	1.22	.942	.985	.996	1.000	1.000
3.912	1.54	.975	.998	1.000	1.000	1.000
4.750	1.87	.991	.997	1.000	1.000	1.000
5.588	2.20	1.000	1.000	1.000	1.000	1.000
6.477	2.55	1.000	1.000	1.000	1.000	1.000
7.493	2.95	1.000	1.000	1.000		
8.839	3.48	1.000	1.000	1.000		
10.160	4.00	1.000	1.000	1.000		
11.430	4.50	1.000	1.000	1.000		
12.700	5.00	1.000	1.000	1.000		

(c) Station 2.62 meters (103 in.)

y		u/ $\bar{U}$ for R equal to -				
cm	in.	0	0.26	0.52	0.78	1.04
0.254	0.10	0.497	0.643	0.776	0.907	1.02
.508	.20	.565	.688	.813	.944	.995
.914	.36	.640	.756	.857	.951	.994
1.194	.47	.687	.796	.888	.966	.993
1.727	.68	.737	.843	.918	.972	.993
2.388	.94	.802	.892	.953	.986	1.000
2.921	1.15	.839	.925	.972	.992	
3.708	1.46	.892	.956	.982	.994	
4.572	1.80	.935	.975	.985	.996	
5.334	2.10	.962	.988	.998	1.000	
6.248	2.46	.972	.986	.994		
7.264	2.86	.986	.995	1.000		
8.636	3.40	.992	.999			
9.982	3.93	1.000	1.000			
12.573	4.95	1.000				

TABLE II.- SUMMARY OF GROSS BOUNDARY-LAYER PARAMETERS  
FROM PROFILE MEASUREMENTS

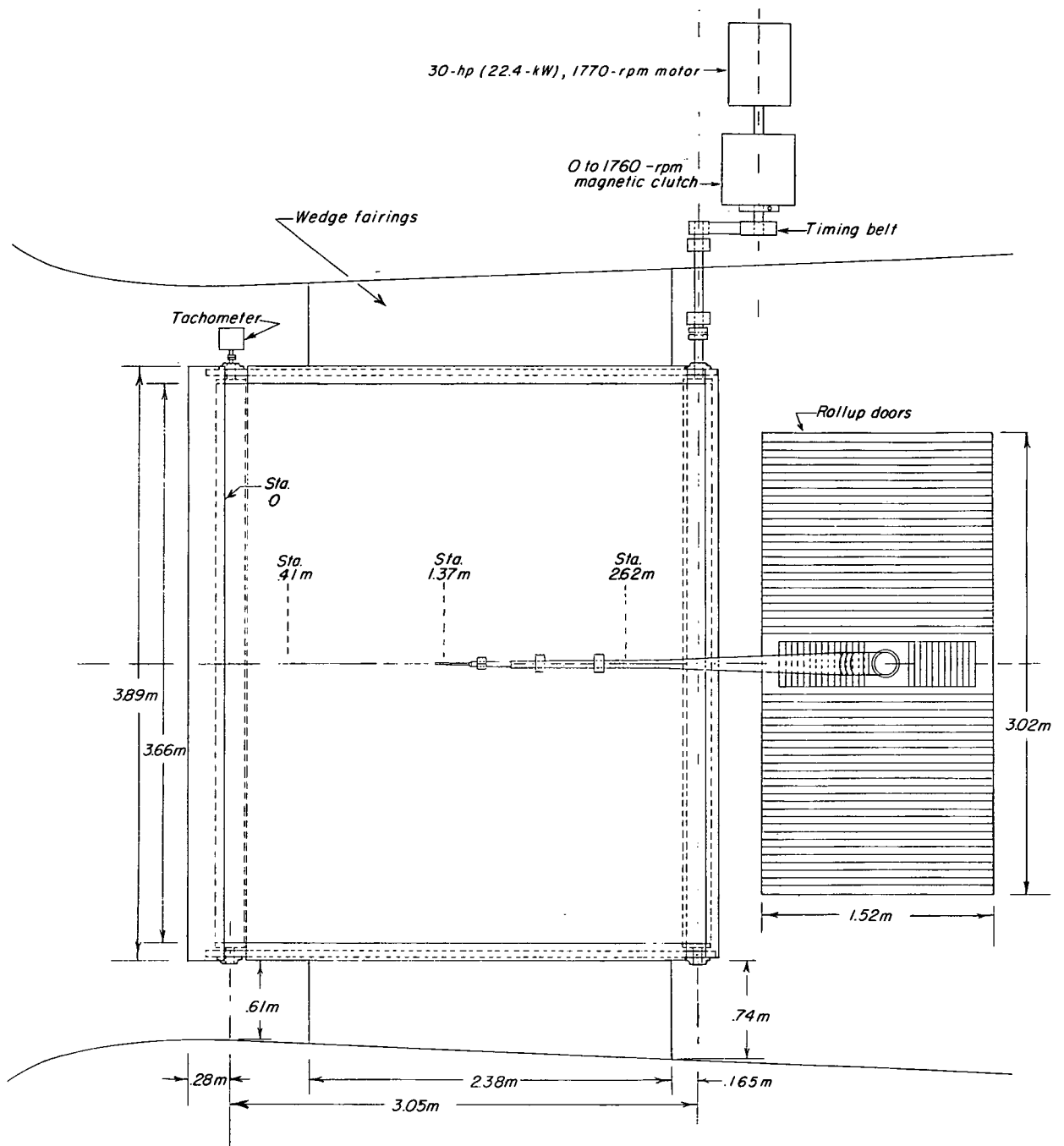
R	$\delta$		$\delta^*$		$\theta$		H	$\tilde{\delta}^*$		$\tilde{\theta}$		$\tilde{H}$
	m	ft	m	ft	m	ft		m	ft	m	ft	
Station 1.37 meters (54 in.)												
0	0.0457	0.150	0.00860	0.0282	0.00546	0.0179	1.58	0.00860	0.0282	0.00607	0.0199	1.58
.26	.0366	.120	.00491	.0161	.00354	.0116	1.39	.00661	.0217	.00415	.0136	1.60
.52	.0293	.096	.00268	.0088	.00216	.0071	1.24	.00558	.0183	.00338	.0111	1.65
.78	.0232	.076	.00107	.0035	.00094	.0031	1.13	.00479	.0157	.00283	.0093	1.69
Station 2.62 meters (103 in.)												
0	0.0732	0.240	0.01204	0.0395	0.00811	0.0266	1.48	0.01204	0.0395	0.00811	0.0266	1.48
.26	.0594	.195	.00698	.0229	.00524	.0172	1.33	.00942	.0309	.00628	.0206	1.50
.52	.0506	.166	.00366	.0120	.00308	.0101	1.19	.00765	.0251	.00509	.0167	1.50
.78	.0427	.140	.00125	.0041	.00116	.0038	1.08	.00570	.0187	.00384	.0126	1.48



(a) Elevation.

Figure 1.- General arrangement of test setup over the moving-belt ground plane.  
 All linear dimensions in meters. (To convert values in meters to inches,  
 multiply by 39.37.)





(b) Plan.

Figure 1.- Concluded.

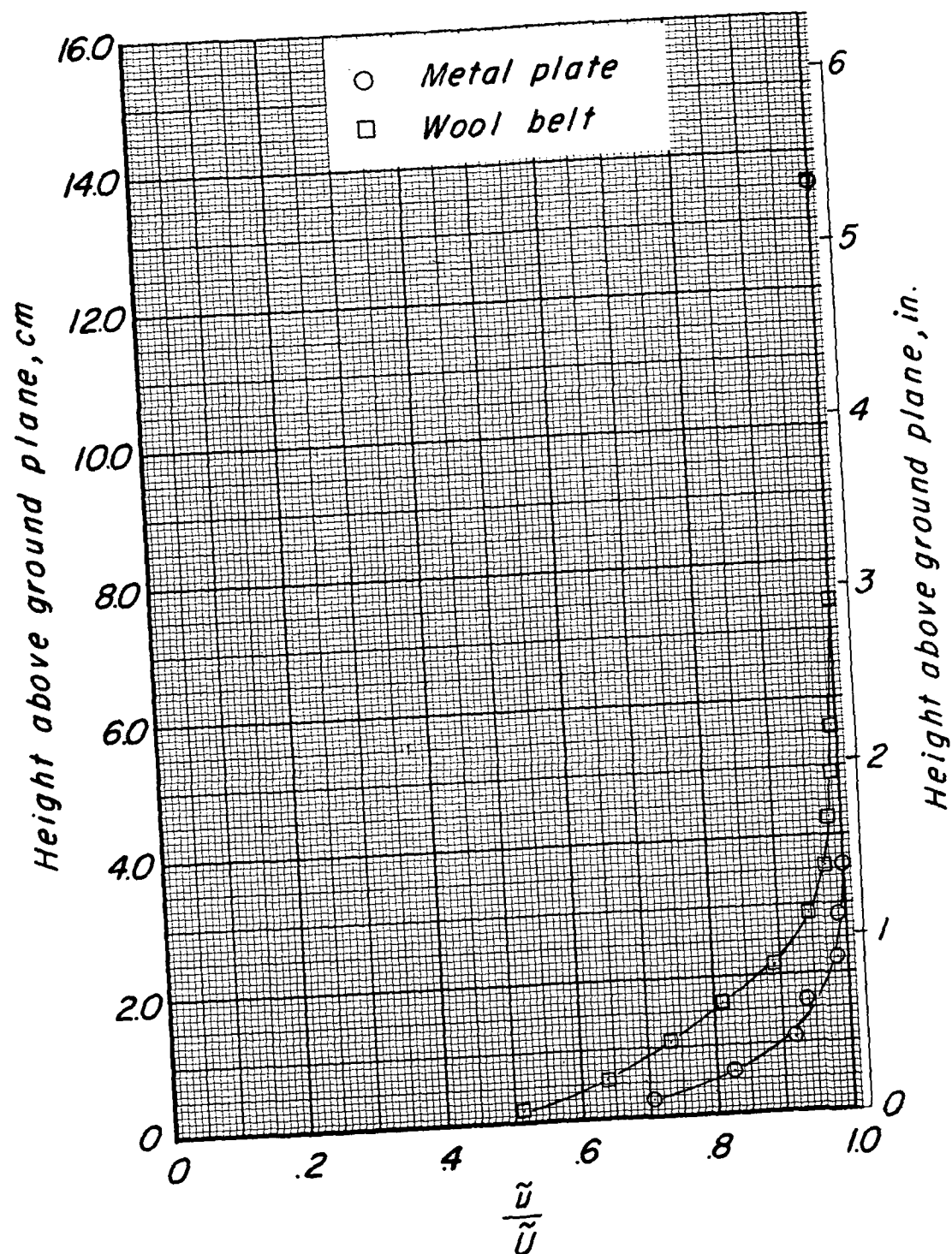
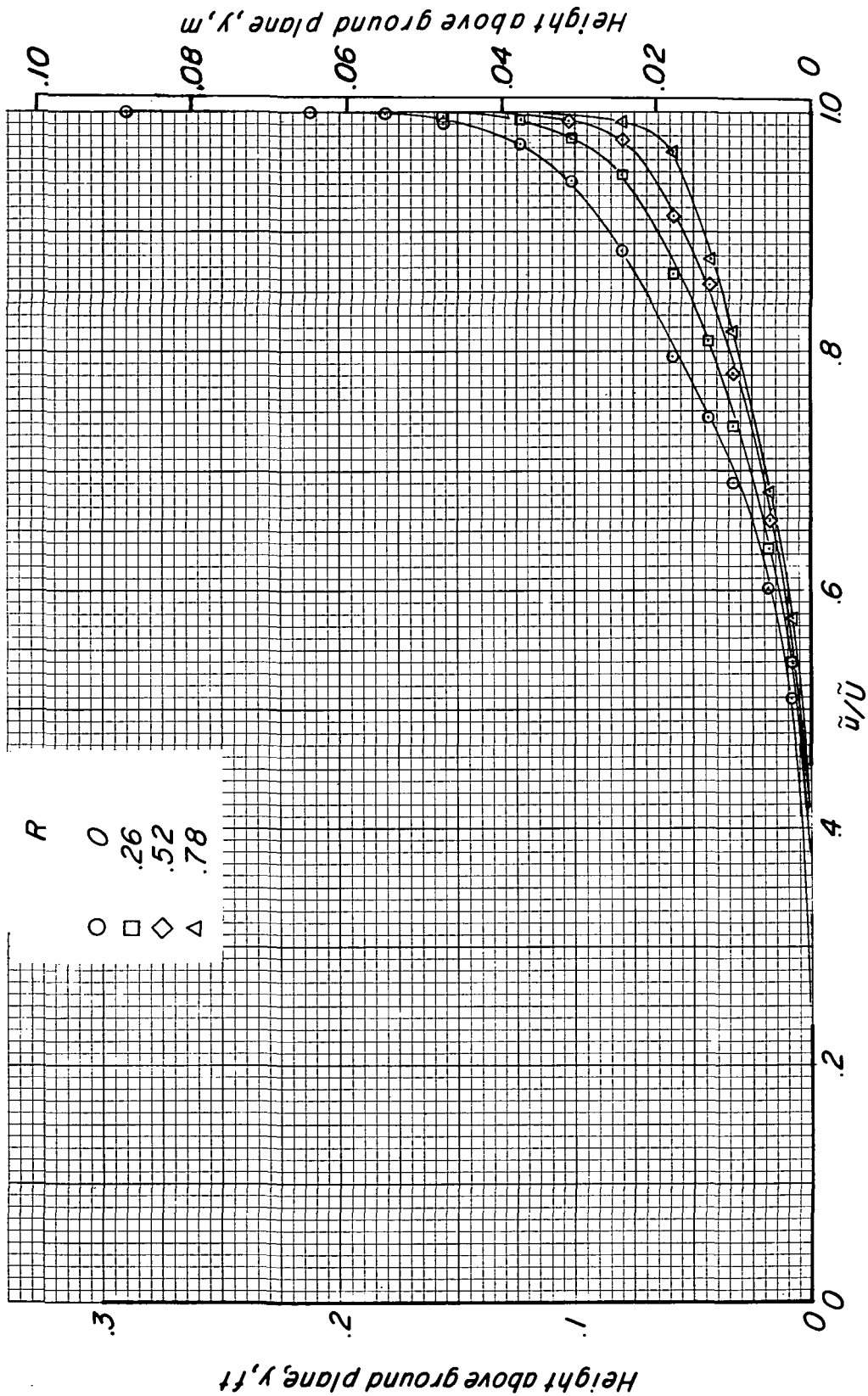
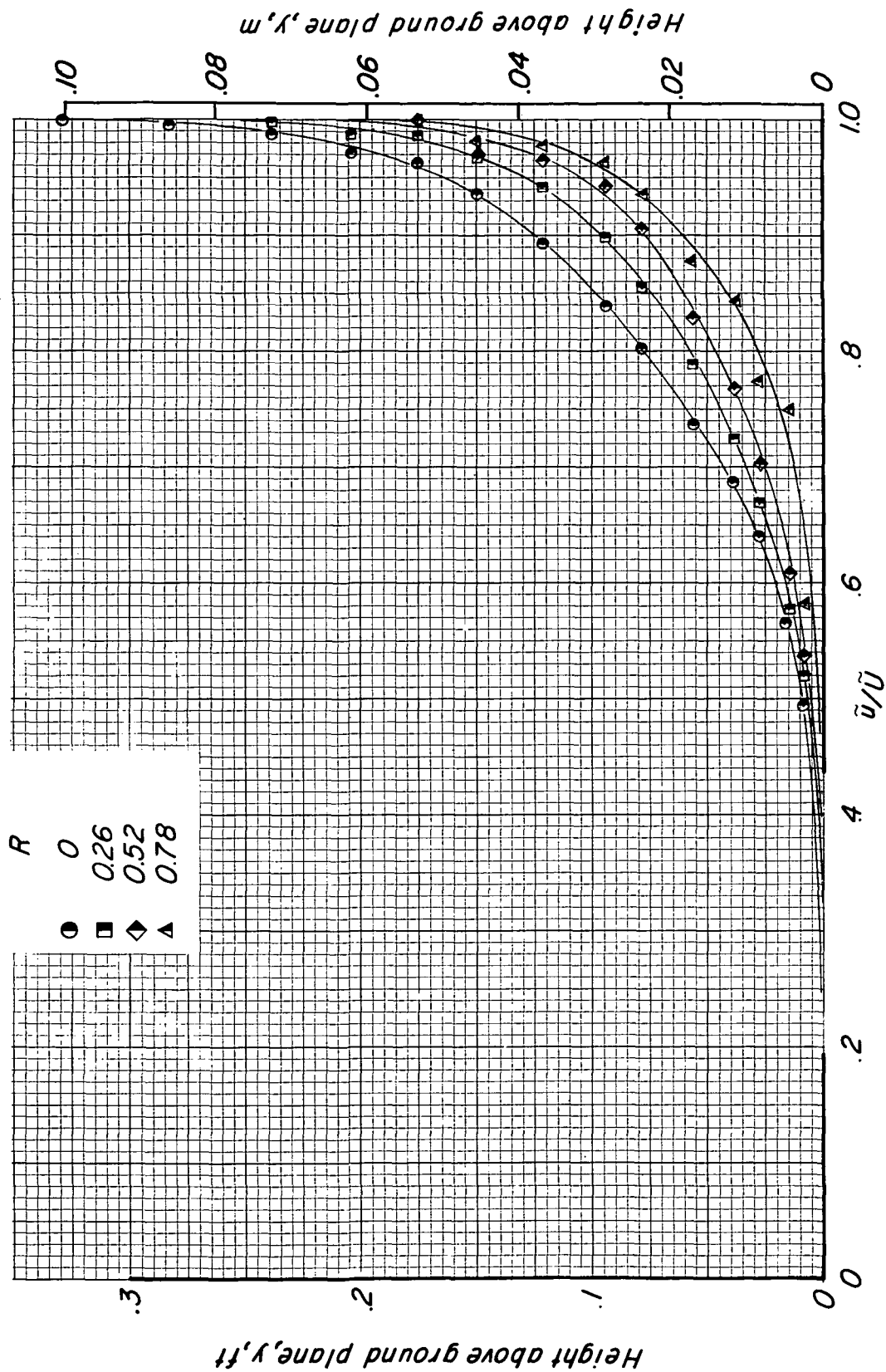


Figure 2.- Boundary-layer profile on belt and on smooth metal plate.  
Station 1.42 meters (56 in.);  $R = 0$ .



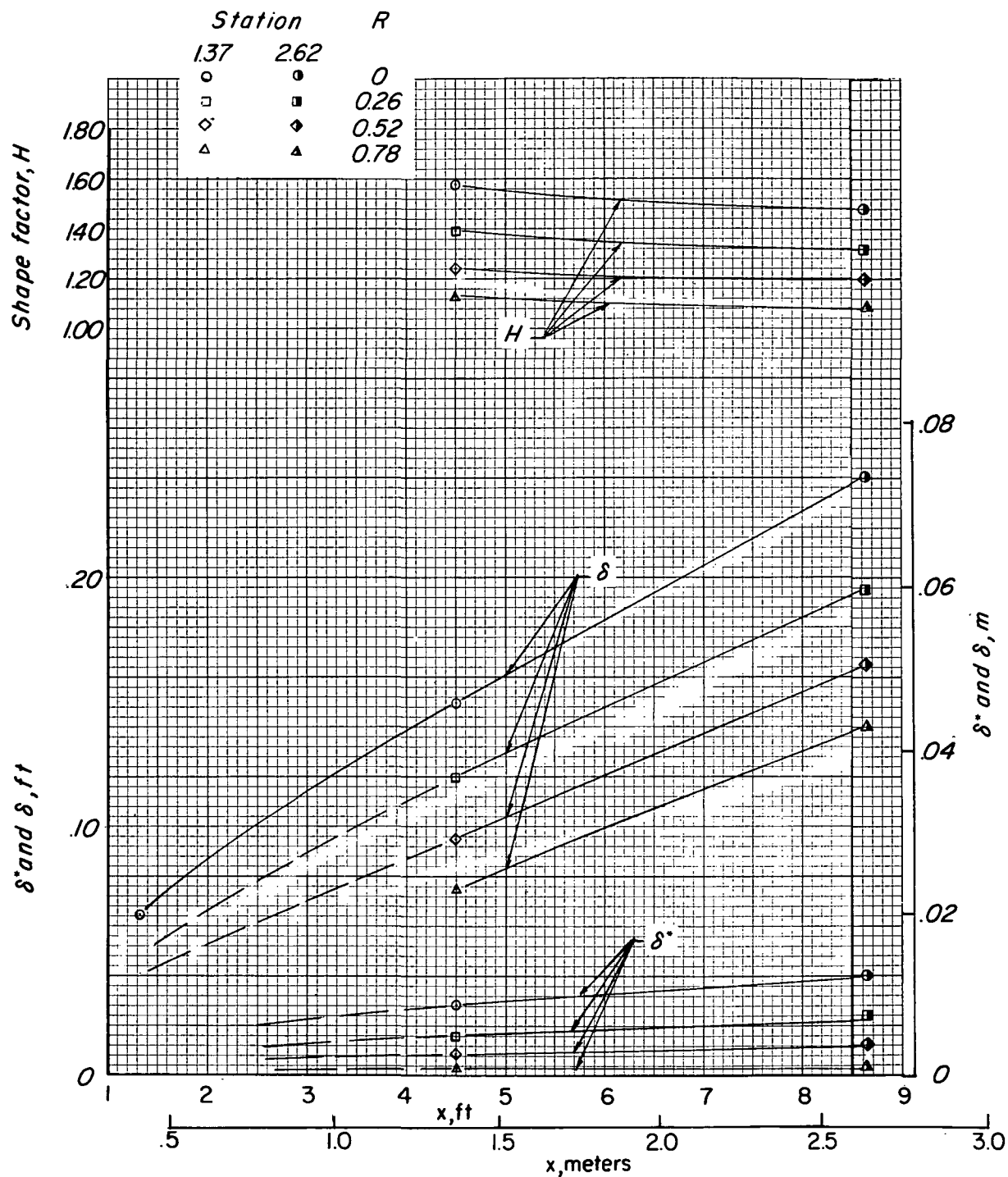
(a) Station 1.37.

Figure 3.- Boundary-layer profile over moving-belt ground plane.



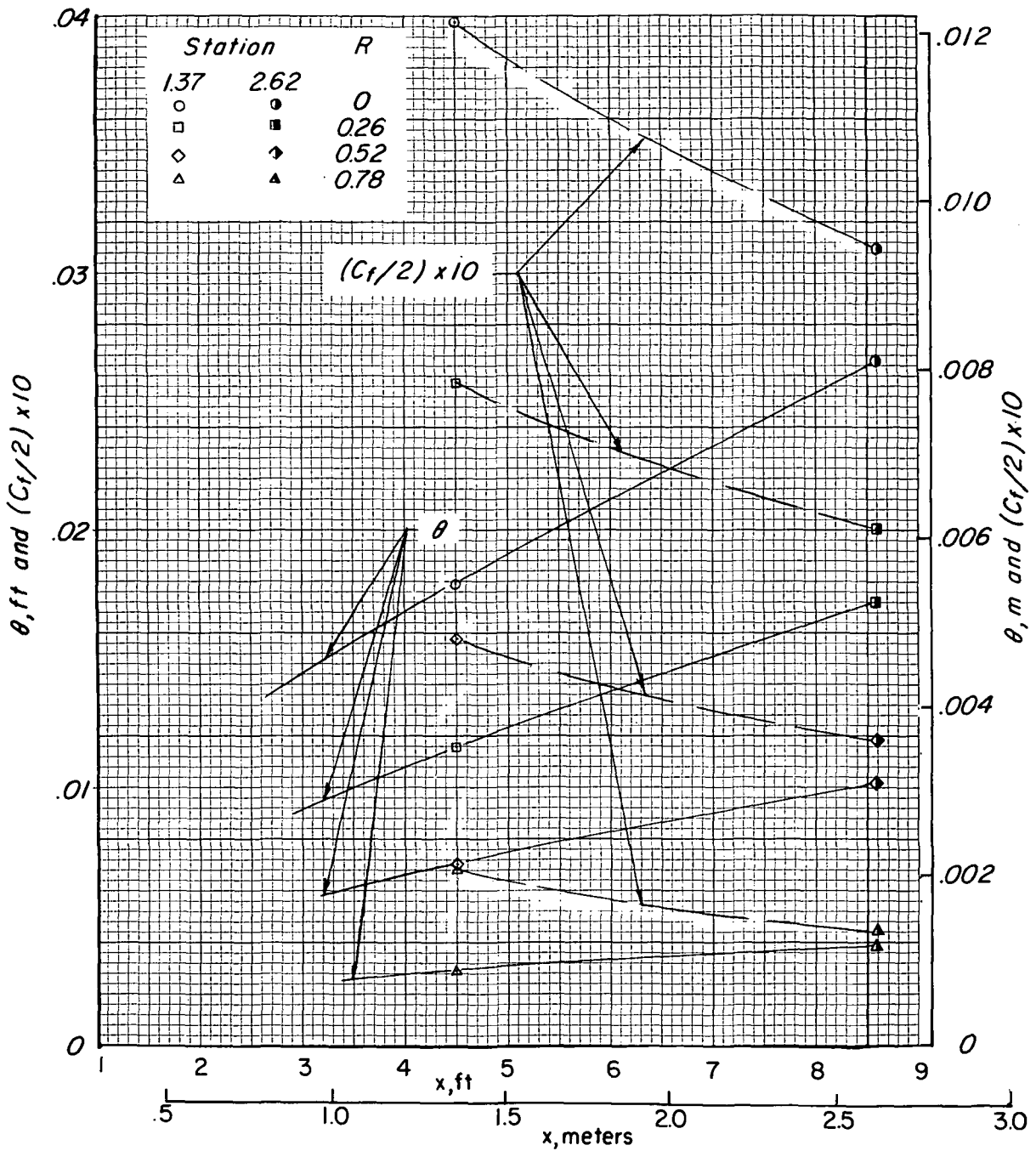
(b) Station 2.62.

Figure 3. - Concluded.



(a)  $\delta$ ,  $\delta^*$ , and  $H$ .

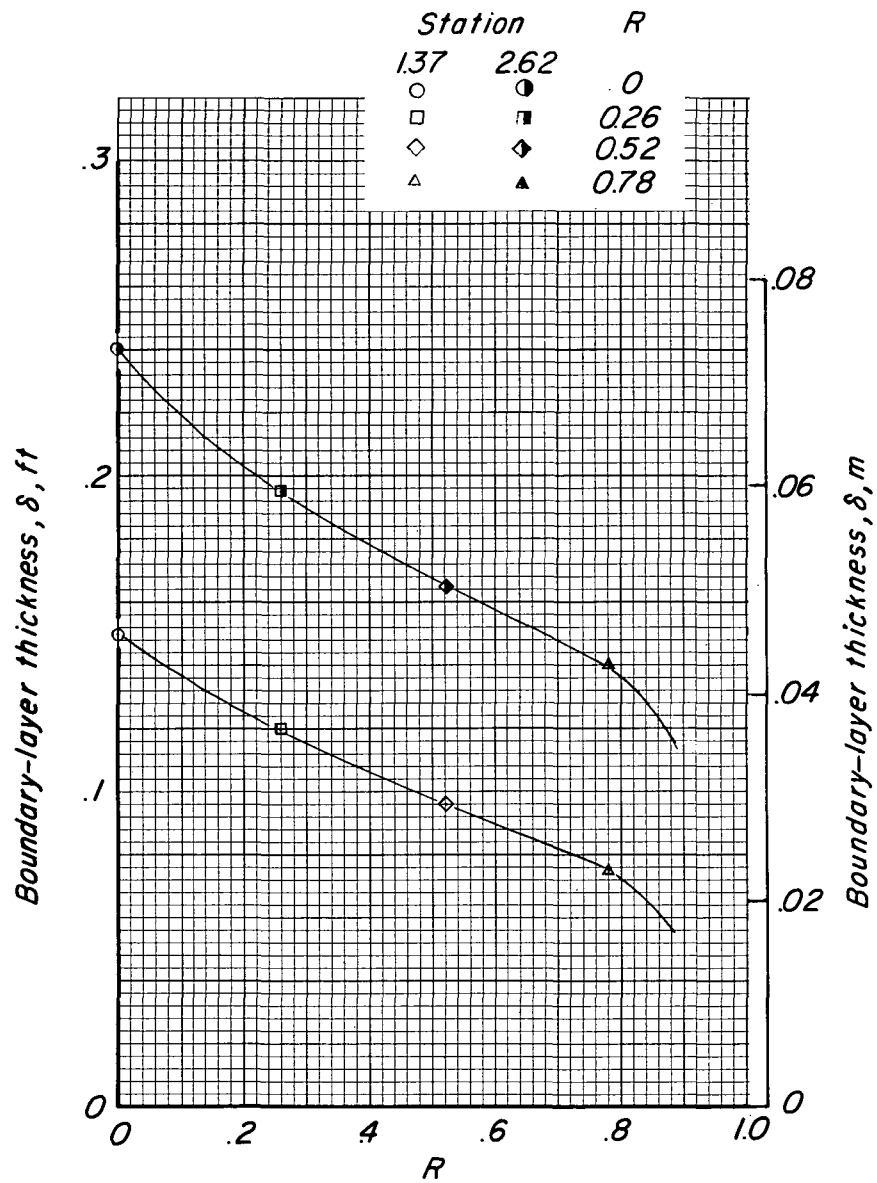
Figure 4.- Variation of boundary-layer parameters with  $x$  over moving-belt ground plane.



(b)  $\theta$  and  $C_f/2$ .

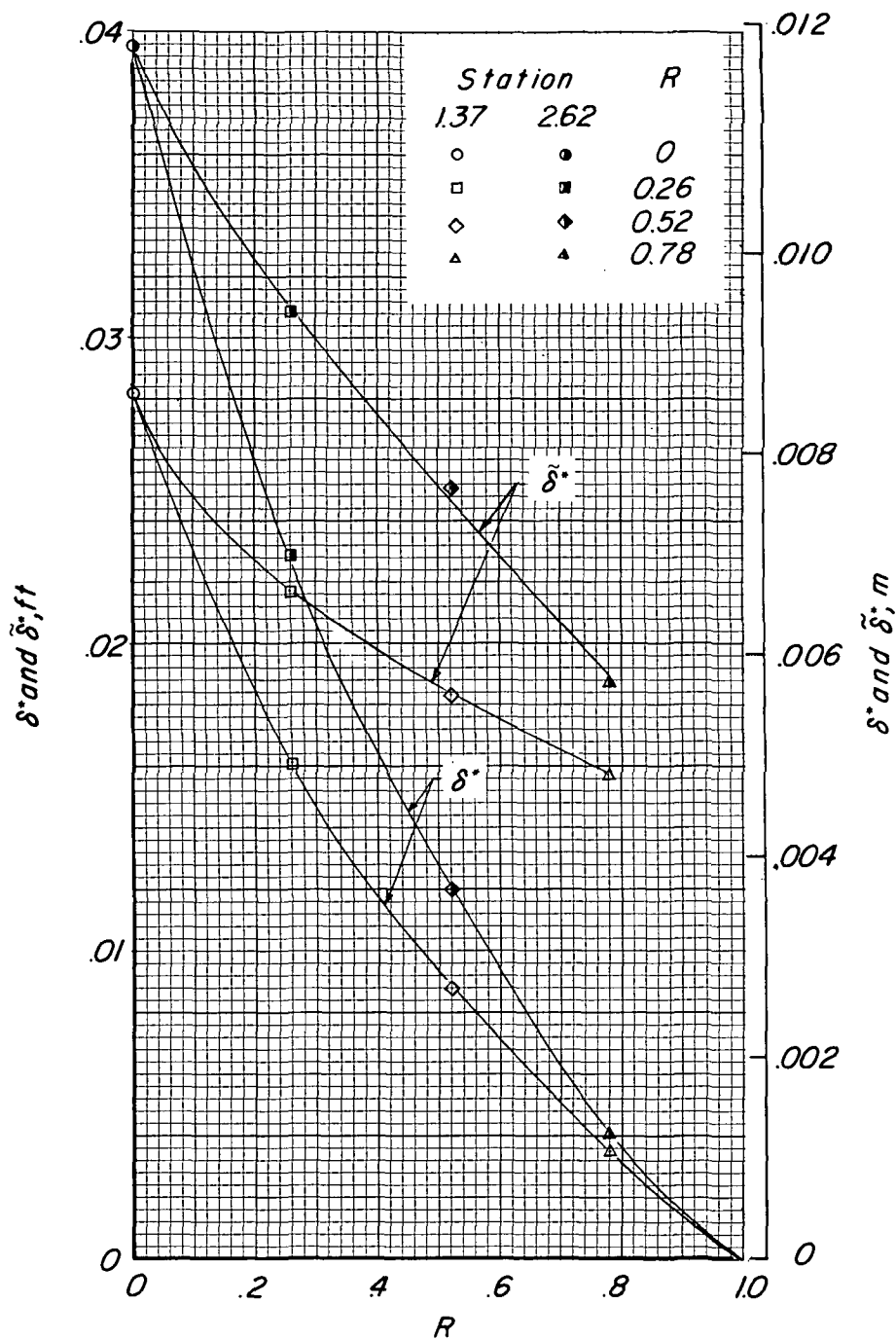
Figure 4.- Concluded.





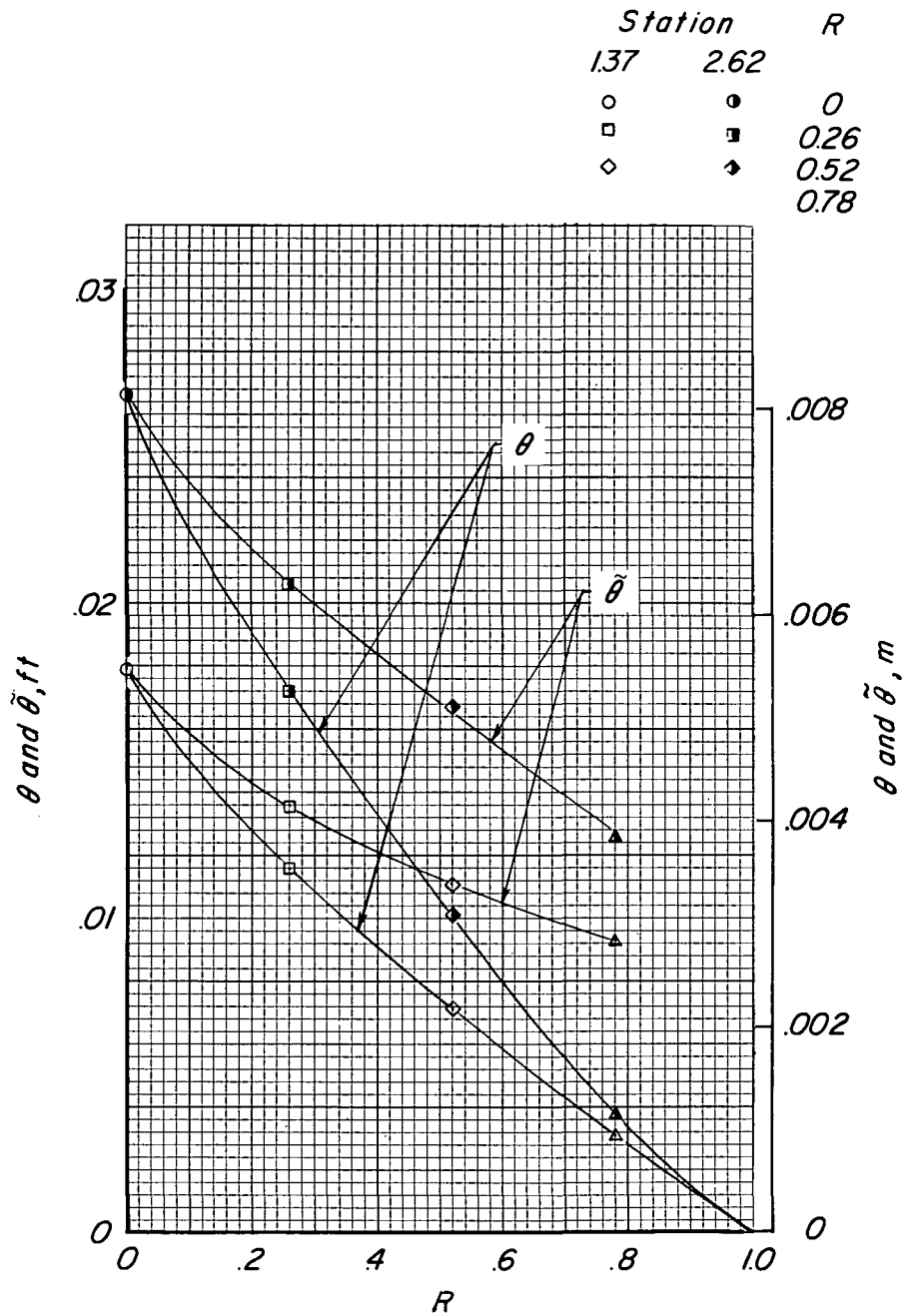
(a) Boundary-layer thickness  $\delta$ .

Figure 5.- Variation of boundary-layer parameters with  $R$ .



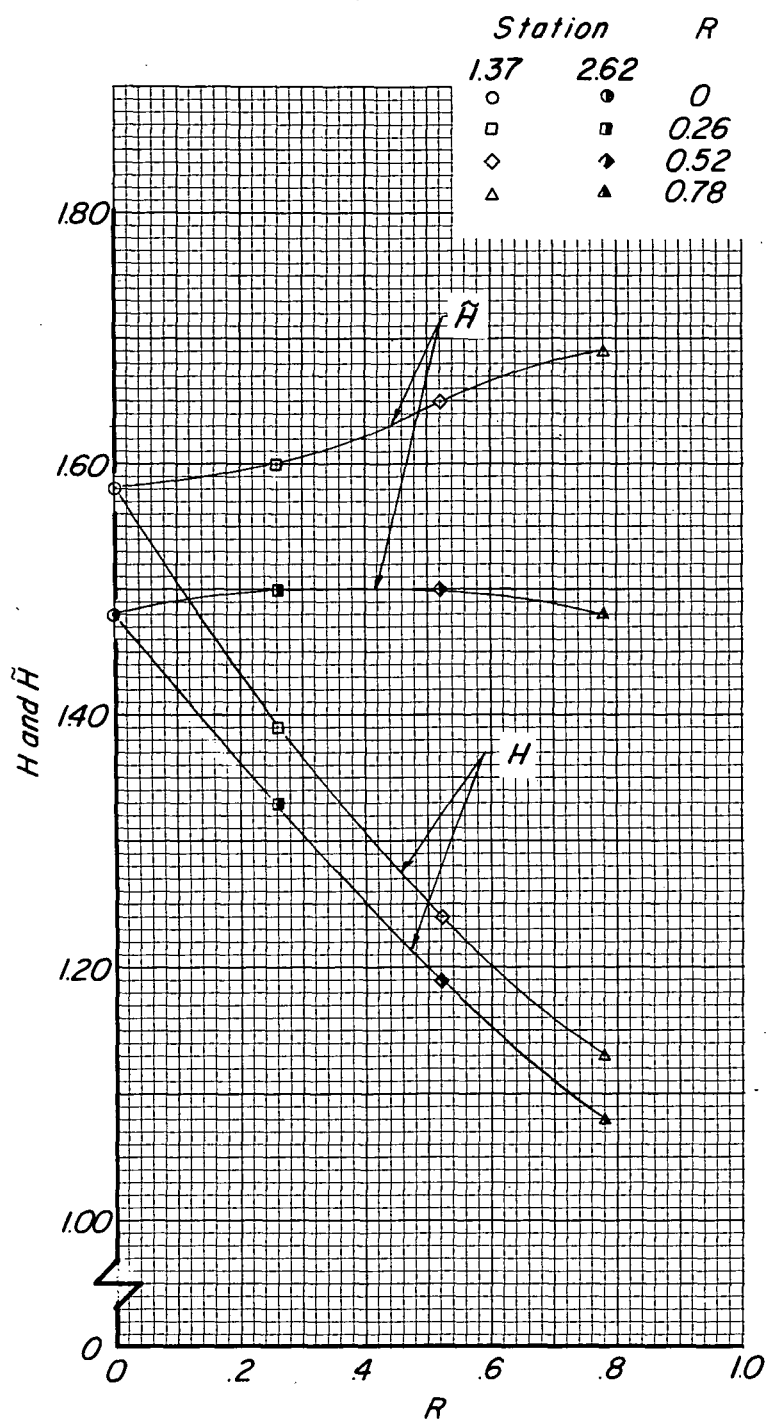
(b)  $\delta^*$  and  $\tilde{\delta}^*$ .

Figure 5.- Continued.



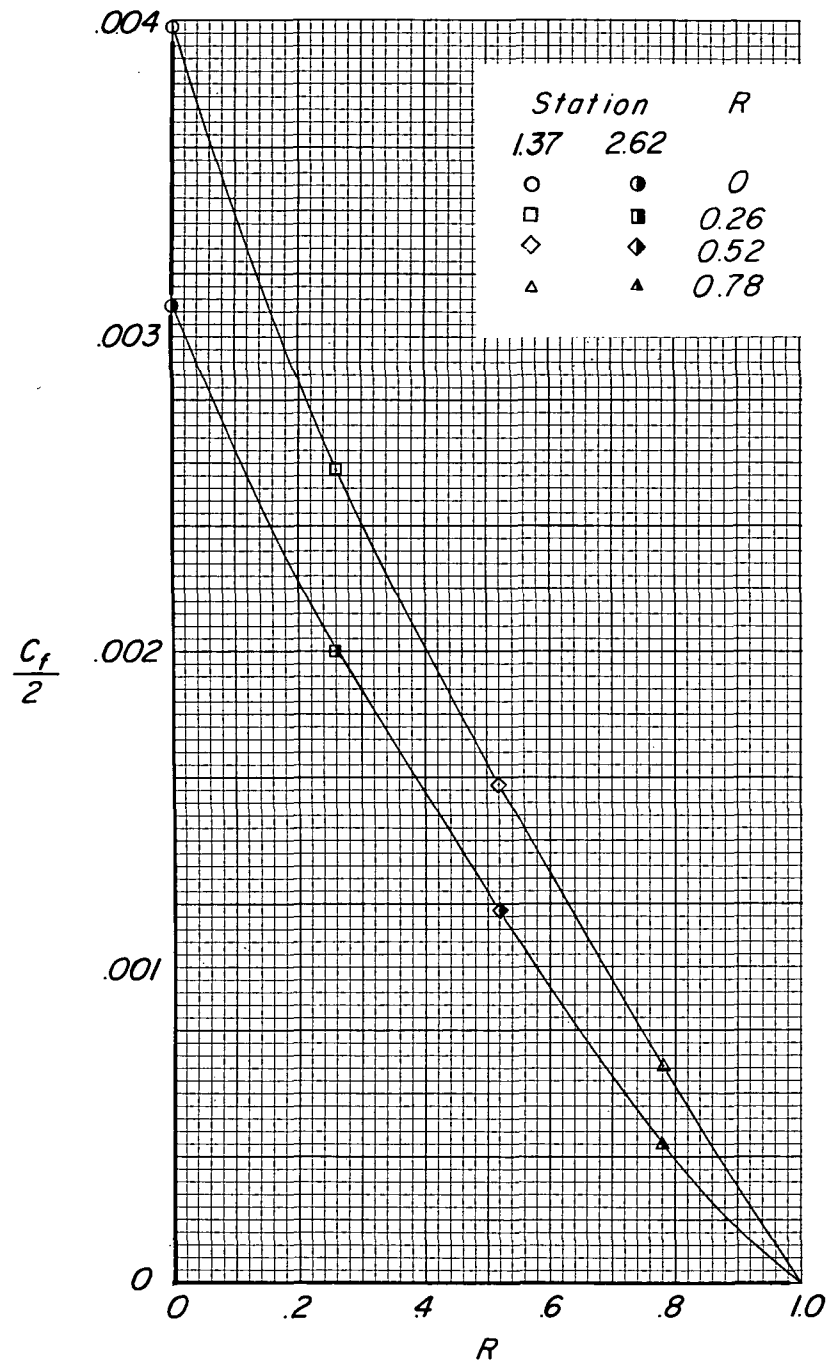
(c)  $\theta$  and  $\tilde{\theta}$ .

Figure 5.- Continued.



(d)  $H$  and  $\tilde{H}$ .

Figure 5.- Continued.



(e) Total skin-friction coefficient.

Figure 5.- Concluded.

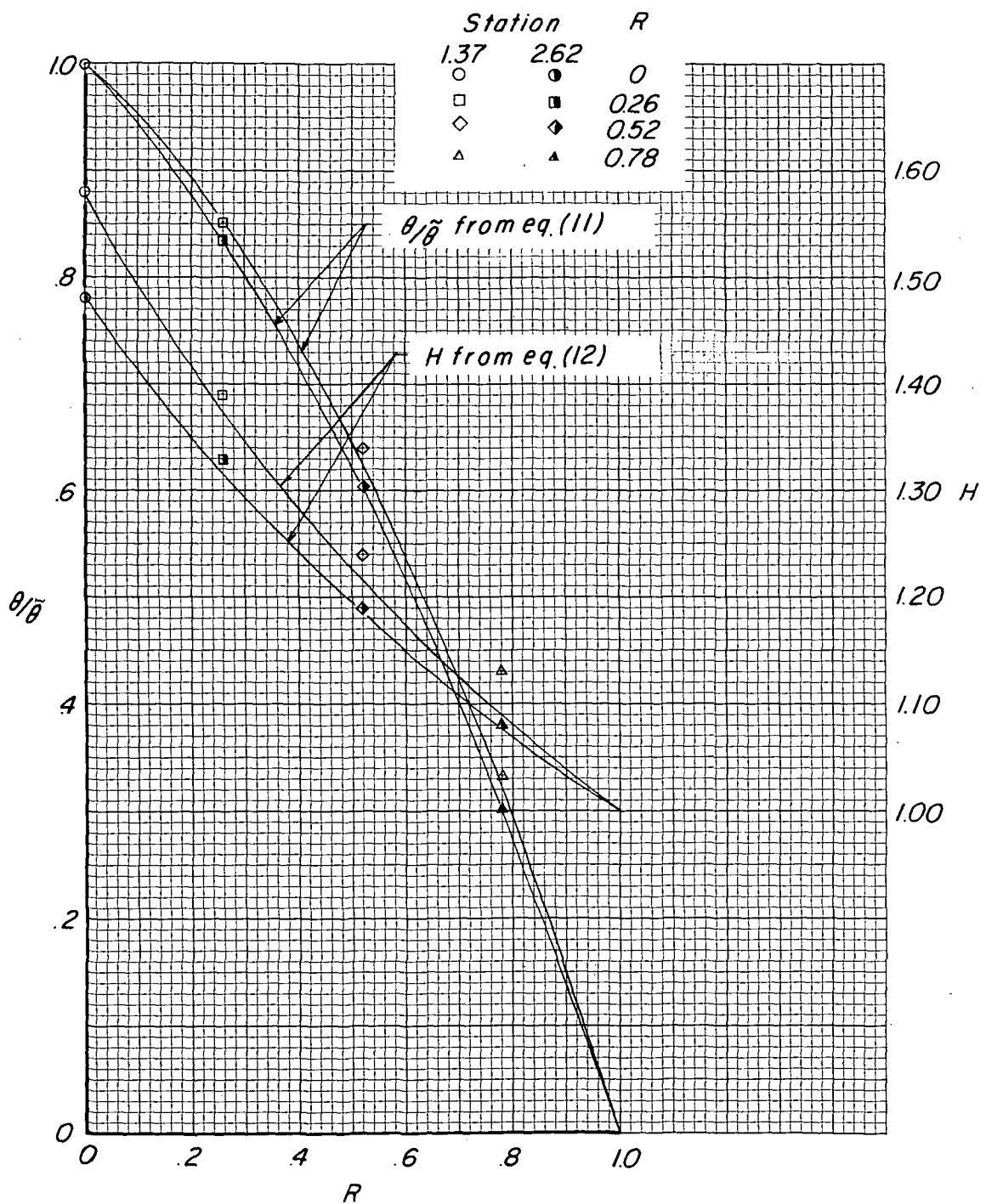


Figure 6.- Comparison of predicted and measured values of  $\theta/\tilde{\theta}$  and  $H$ .



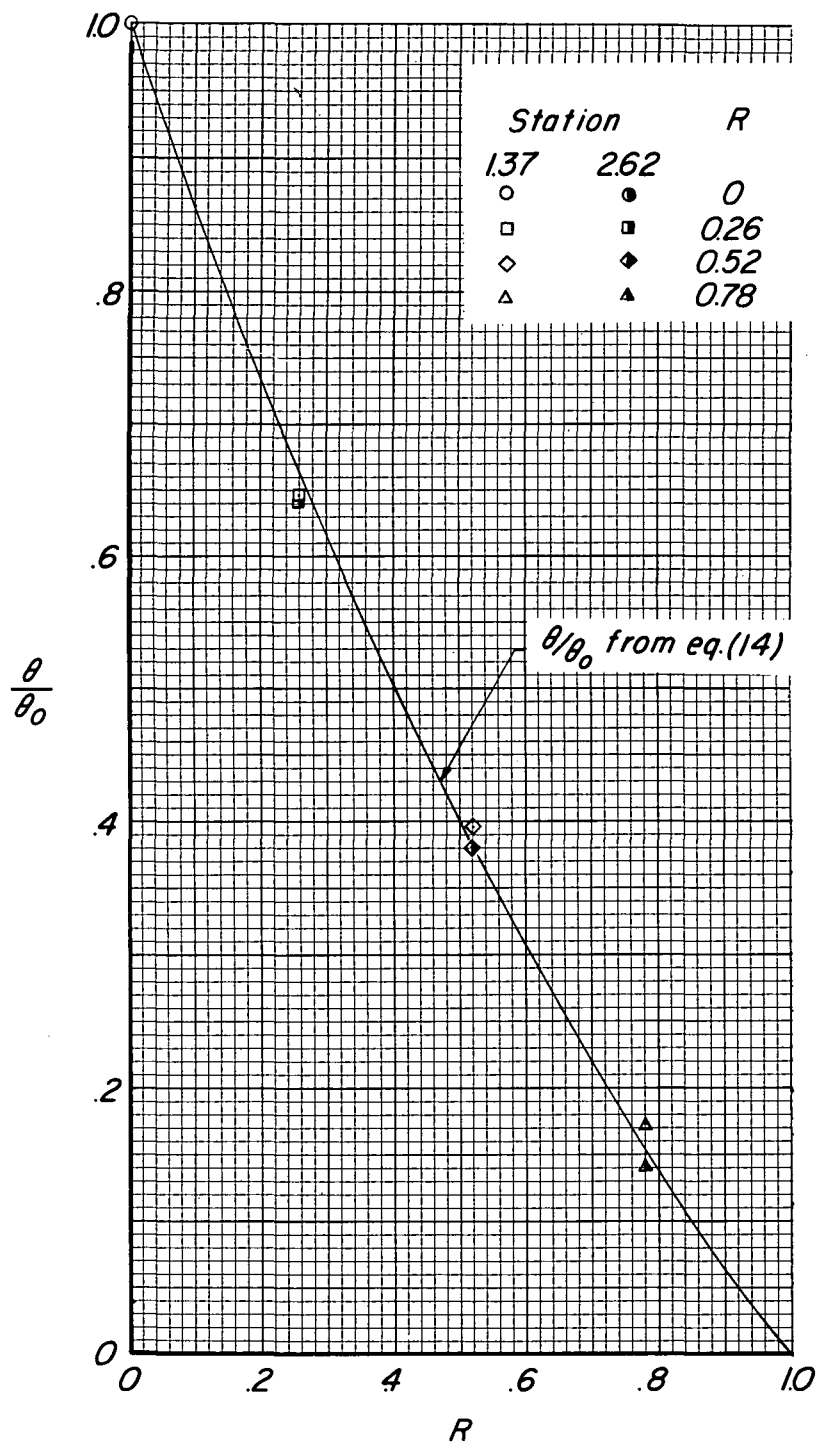


Figure 7.- Comparison of predicted and measured values of  $\theta/\theta_0$ .

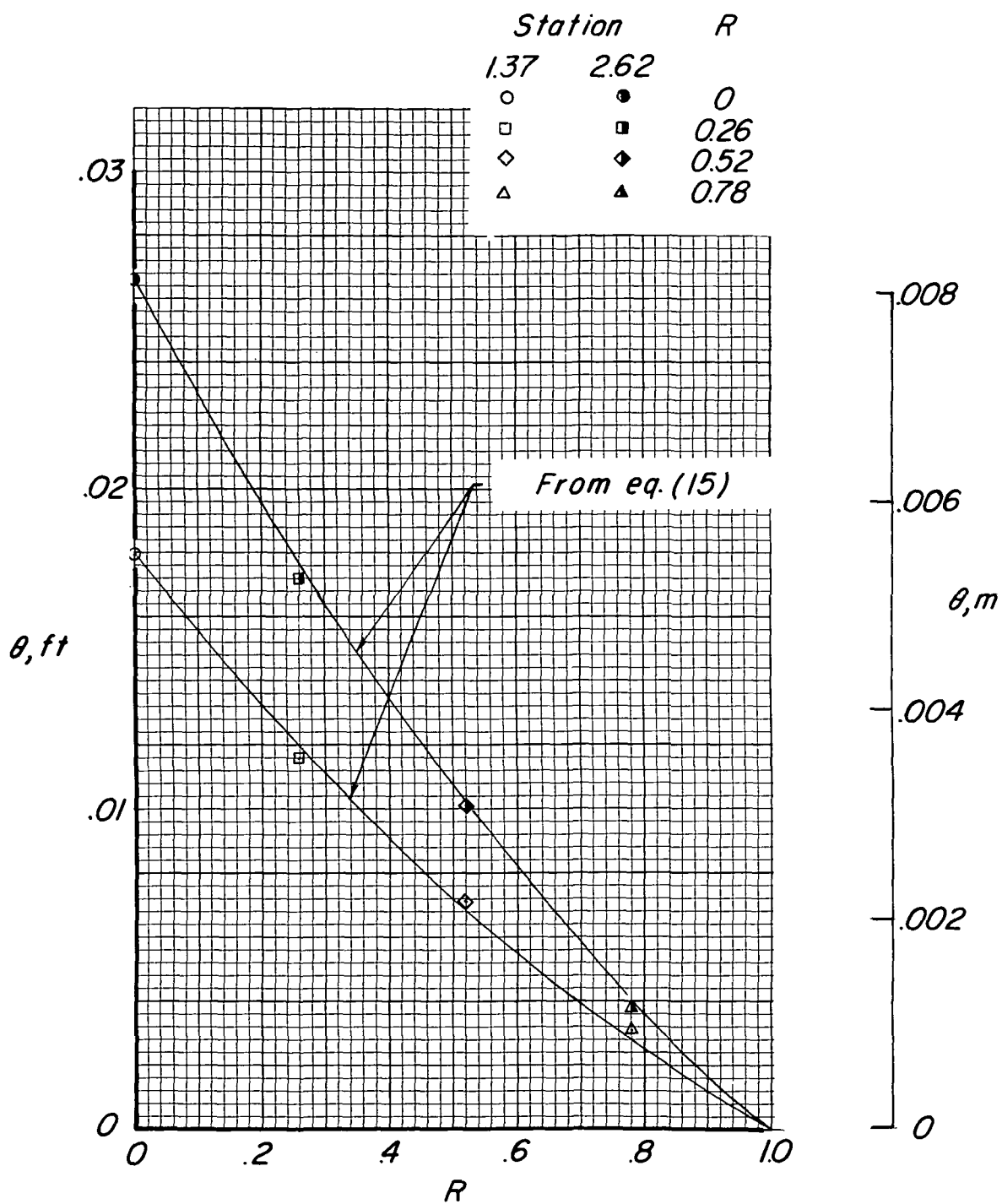


Figure 8.- Comparison of predicted and measured values of  $\theta$ .

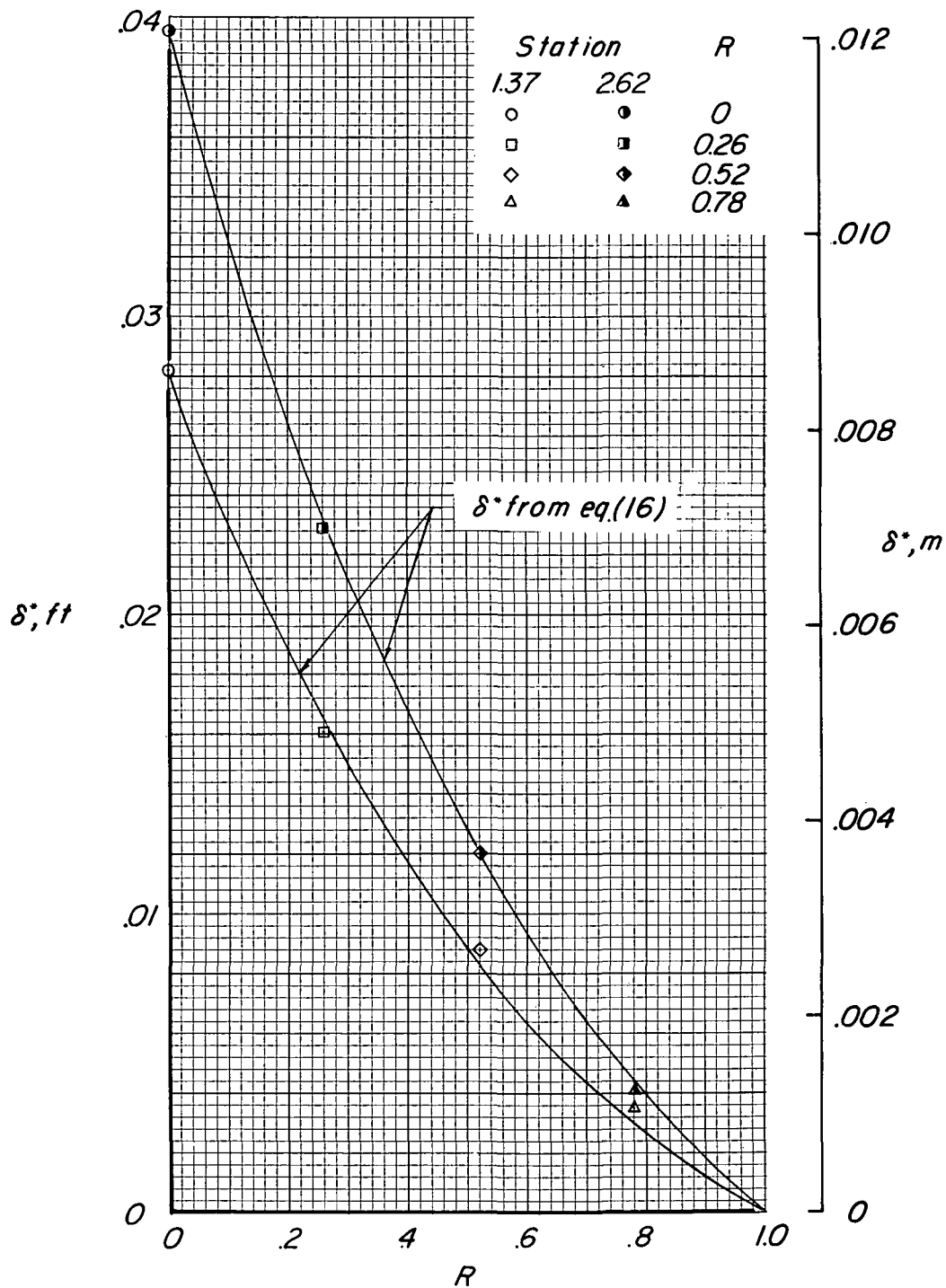


Figure 9.- Comparison of predicted and measured values of  $\delta^*$ .



POSTMASTER: If Undeliverable (Section 158  
Postal Manual) Do Not Return

*"The aeronautical and space activities of the United States shall be conducted so as to contribute . . . to the expansion of human knowledge of phenomena in the atmosphere and space. The Administration shall provide for the widest practicable and appropriate dissemination of information concerning its activities and the results thereof."*

—NATIONAL AERONAUTICS AND SPACE ACT OF 1958

## NASA SCIENTIFIC AND TECHNICAL PUBLICATIONS

**TECHNICAL REPORTS:** Scientific and technical information considered important, complete, and a lasting contribution to existing knowledge.

**TECHNICAL NOTES:** Information less broad in scope but nevertheless of importance as a contribution to existing knowledge.

**TECHNICAL MEMORANDUMS:** Information receiving limited distribution because of preliminary data, security classification, or other reasons.

**CONTRACTOR REPORTS:** Scientific and technical information generated under a NASA contract or grant and considered an important contribution to existing knowledge.

**TECHNICAL TRANSLATIONS:** Information published in a foreign language considered to merit NASA distribution in English.

**SPECIAL PUBLICATIONS:** Information derived from or of value to NASA activities. Publications include conference proceedings, monographs, data compilations, handbooks, sourcebooks, and special bibliographies.

**TECHNOLOGY UTILIZATION PUBLICATIONS:** Information on technology used by NASA that may be of particular interest in commercial and other non-aerospace applications. Publications include Tech Briefs, Technology Utilization Reports and Technology Surveys.

*Details on the availability of these publications may be obtained from:*

**SCIENTIFIC AND TECHNICAL INFORMATION OFFICE**

**NATIONAL AERONAUTICS AND SPACE ADMINISTRATION**

Washington, D.C. 20546